Endoprotease-Mediated Intracellular Protein Delivery Using Nanocapsules

Anuradha Biswas,[†,§] Kye-Il Joo,[#] Jing Liu,[∥] Muxun Zhao,[†,§] Guoping Fan,[∥] Pin Wang,[#] Zhen Gu,[†,§,⊥,▽,*] and Yi Tang[†,§,‡,*]

[†]Department of Chemical and Biomolecular Engineering, [‡]Department of Chemistry and Biochemistry, [§]California NanoSystems Institute, [⊥]Department of Mechanical and Aerospace Engineering, and [∥]Department of Human Genetics, University of California at Los Angeles, Los Angeles, California 90095, United States, and [#]Mork Family Department of Chemical Engineering and Materials Science, University of Southern California, Los Angeles, California 90089, United States. [▽] Current address: Koch Institute for Integrative Cancer Research, Massachusetts Institute of Technology, Cambridge, Massachusetts 02139.

ABSTRACT Proteins possess distinct intracellular roles allowing them to have vast therapeutic applications. However, due to poor cellular permeability and fragility of most proteins, intracellular delivery of native, active proteins is challenging. We describe a biomimetic protein delivery vehicle which is degradable upon the digestion by furin, a ubiquitous intracellular protease, to release encapsulated cargos. Proteins were encapsulated in a nanosized matrix prepared with monomers and a bisacrylated peptide cross-linker which can be specifically recognized and cleaved by furin. Release of encapsulated protein was confirmed in a cell-free system upon proteolytic degradation of nanocapsules. *In vitro* cell culture studies demonstrated successful intracellular delivery of both nuclear and cytosolic proteins and confirmed the importance of furin-degradable construction for native protein release. This endoprotease-mediated intracellular delivery system may be extended to effectively deliver various biological therapeutics.

KEYWORDS: protein delivery · nanocapsule · intracellular · polymer · endoprotease

Proteins are the engines of life by performing essential functions, such as catalysis, signal transduction, and gene regulation, and maintaining a fine balance between cell survival and programmed death.[1] Consequently, intracellular delivery of functional proteins has significant therapeutic implications in biological applications, including disease therapies, vaccination, and imaging.[2] However, the poor stability and membrane impermeability of most native proteins make efficient delivery difficult. Different strategies that aim to protect protein integrity and activity as well as to aid intracellular delivery have been explored. Covalent approaches include genetic fusion of protein transduction domains[3,4] and conjugation of polymers to free amine groups on the surface of proteins.[5−7] However, these approaches often suffer from alteration of protein activity due to modification of protein structure. Noncovalent-based polymer carriers that encapsulate protein cargo *via* electrostatic assembly[8,9] or hydrophilic and hydrophobic interactions have also been explored.[10,11] These methods employ various materials to effectively help the protein travel into cells, albeit often suffer from instability in serum.

Polymer carriers can be engineered to release cargo after cellular entry by employing a degradable moiety triggered by an external or cellular signal.[12,13] These strategies allow protein to be protected during cellular entry through the negatively charged phospholipid bilayer membrane and degrade to expose native protein once inside the cell in response to different cellular environments. Degradation of the polymer carrier has been engineered to respond to lowered pH in endosomal compartments,[14,15] higher levels of reducing agent glutathione in the cytosol,[16] and hydrolysis by nonspecific esterases in the cytosol.[17,18] Despite these significant efforts, a controlled release mechanism that is based on specific actions of cellular enzymes is highly attractive because of the exquisite selectivity and the neutral pH degradation conditions.[19] Recent advances have utilized secreted and membrane-associated proteases, such as matrix metalloproteinases (MMPs), to degrade polymers and release cargo in extracellular space from hydrogels.[20,21] To achieve delivery of native proteins, we recently reported a strategy to first protect and then remove the protective coating intracellularly without affecting protein function.[22] We demonstrated intracellular delivery of apoptotic protease caspase-3 (CP3) encapsulated in polymer nanocapsules (NCs) that are cross-linked with peptides that can be degraded by CP3 from within. Although effective as an apoptosis-inducing NC, the strategy is specialized by the requirement that the cargo

*Address correspondence to guzhen@mit.edu, yitang@ucla.edu.

Received for review November 15, 2010 and accepted January 7, 2011.

Published online
10.1021/nn1031005

itself must be proteolytically active to degrade the protective shell.

In order to deliver a wide assortment of functional proteins that can interact with different cellular targets, a general mechanism for enzymatic degradation of the NC and release of the protein cargo is needed. Toward this end, we sought to design the NC that can disintegrate and release proteins in response to the essential endoprotease furin (53 kDa), which is an ubiquitous proprotein convertase expressed in all eukaryotic organisms and many mammalian cells.[23,24] Furin is localized in various intracellular locations and has a preferred substrate in the form RX(K/R)R↓ (R: arginine; K: lysine, X: any amino acid; ↓: the cleavage site).[25] Furin processes a diverse group of endogenous proproteins and foreign proteinaceous substrates, including those from bacterial toxins, such as Shiga toxins and anthrax as well as many viruses, such as measles and HIV-1. A previous study elucidated the significance of a furin-mediated cleavage of the papillomavirus (PV) minor capsid protein L2 for necessary dissociation of the capsid, release of viral DNA, and subsequent transfections.[26] We were motivated by these existing natural roles of furin, both in the maturation of cellular proteins and the activation of foreign invaders. We demonstrate here the design and synthesis of a furin-degradable biomimetic protein delivery vehicle that can successfully deliver both cytosolic and nuclear proteins in active forms to a variety of cell lines.

RESULTS AND DISCUSSION

Physical Characterization of Protein NCs. The biomimetic design of our NC was inspired from how natural foreign delivery vehicles, such as viruses, utilize furin to cleave their protective layers leading to release of invading cargo.[27] Furin-mediated processing of these viruses allows the mature viral envelope to become exposed or leads to disintegration of the capsid, thereby leading to successful transfections. Our strategy was to noncovalently encapsulate the target protein cargo in a thin, positively charged polymer layer, using two monomers and furin-cleavable peptides as cross-linkers (CLs) (Figure 1A). The peptidyl cross-linkers are analogous to various furin substrates, such as the PV L2 capsid protein. Upon entry into the cell, where furin activities are abundant at various intracellular locations, the CLs are proteolyzed and the polymeric matrix degrades, leading to the release of cargo in native form (Figure 1B).

We selected a highly favored furin substrate (RVRR) and synthesized a bisacrylated peptide CL (Ahx-RVRRSK) as the NC CL, as shown in Scheme S1, Supporting Information.[28,29] Fmoc chemistry was used to synthesize a peptide with 6-aminohexanoic acid (Ahx) at the N-terminus and a methyltrityl (Mtt)-protected lysine residue at the C-terminus. After selective deprotection and cleavage of the Mtt protection group with 3% trifluoroacetic acid (TFA), the peptide was bisacrylated using acryolyl chloride. This strategy, which utilized differential acid-labile protection groups on the side chains of amino acids to synthesize the CL, allowed acryolation of only the N- and C-terminal free amine groups while preserving the arginine groups unmodified for furin recognition. Additionally, complete synthesis on amide resin resulted in high yield and purity of the final peptide product. The CL was purified with high-performance liquid chromatography (HPLC) and characterized by liquid chromatography mass spectrometry (LCMS) analysis (*m/z*: $[M + 2H]^{2+} = 511$; $[M + 3H]^{3+} = 341$; expected molecular weight: 1021). Upon incubation with 1 unit of furin, complete cleavage of 1 ng peptide was observed within 2 h (Figures S1 and S3, Supporting Information). To prepare the protein-containing NCs, monomers acrylamide (AAm) and positively charged *N*-(3-aminopropyl) methacrylamide (APMAAm) and CLs (Figure 1A) were first physically adsorbed onto the surface of the target protein, which included enhanced green fluorescence protein (eGFP), caspase-3 (CP3), bovine serum albumin (BSA), or the transcription factor Klf4, in this study. This was followed by *in situ* free radical interfacial polymerization to form the polymeric shell and to assemble the NC, which can disintegrate and release cargo upon furin cleavage.

The sizes of NCs were assessed to be between 10 and 15 nm by dynamic light scattering (DLS) (Table S1, Figure S4, Supporting Information). The NCs displayed positive ζ potential of 7−9 mV (Table S1, Supporting Information), which is desired for enhanced intracellular uptake.[30,31] To evaluate the furin-degradable property of the synthesized NCs, we first examined NCs using transmission electron microscopy (TEM) and observed furin-degradable eGFP NCs to have a compact, spherical shape. In contrast, after 10 h incubation with furin (1 unit), the NCs appeared completely dissociated, less robust, and were indistinguishable from native eGFP (Figure 1C and D). To confirm that the structural integrity of protein remained intact during NC synthesis and furin digestion, we performed circular dichroism (CD) to examine eGFP before and after NC degradation. CD spectra indicated that the secondary structure of eGFP remained unchanged during the entire NC assembly and disintegration process and was identical to that of native eGFP in solution (Figure S5, Supporting Information).

We then quantified the release of eGFP from NCs using the enzyme-linked immunosorbant assay (ELISA), since only released native eGFP is able to bind to anti-GFP antibody, while encapsulated eGFP is unable to be recognized by the antibody. In addition to furin-degradable NCs, we also examined protein release from nondegradable NCs that were cross-linked using *N,N′*-methylene bisacrylamide. In the absence of furin, degradable NCs did not display significant protein release over a period of 24 h (Figure 1E), which was comparable to that of nondegradable NCs. This indicates that eGFP can remain encapsulated in the polymeric shell

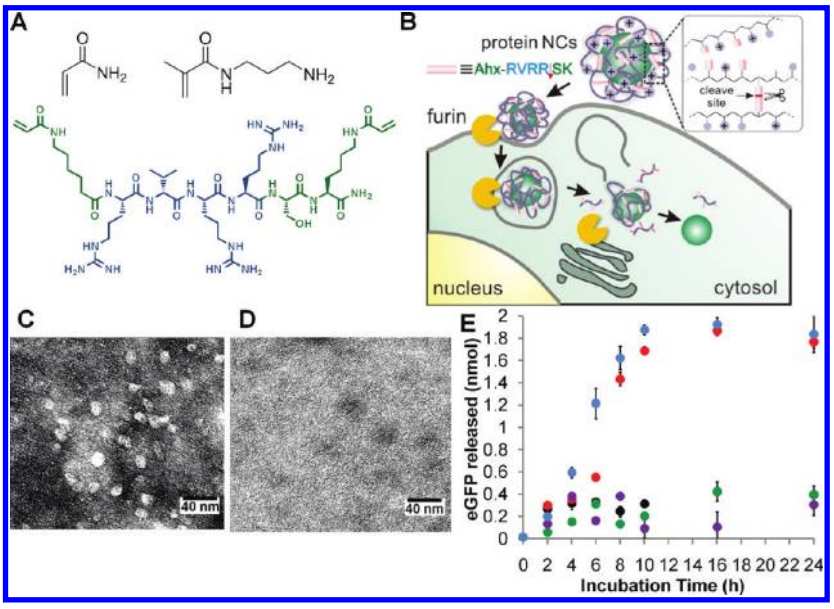

Figure 1. Schematics and physical characterization of degradable NCs. (A) Structure of monomers, acrylamide and *N*-(3-aminopropyl) methacrylamide, and synthesized furin-degradable CL used to form NCs. (B) Monomers and furin-degradable CLs are polymerized to create a degradable polymeric matrix around protein. NCs degrade intracellularly and protein releases upon proteolysis of the CLs by furin. (C) TEM images of fresh NCs and (D) NCs after incubation with furin for 10 h. (E) eGFP release by 2.5 nmol NCs for 10 h. Black solid circle: Furin-degradable NCs; Furin-degradable NCs with 1 U (red solid circle) and 4 U (blue solid circle) furin; Green solid circle: Furin-degradable NCs with 1 U furin and dec-RVKR-cmk; and purple solid circle: NCs with nondegradable CLs. The data represent averages with error bars from three independent experiments.

over an extended period of time and that protein diffusion effects are negligible. In contrast, upon addition of 1 unit furin to furin-degradable NCs, a steady increase (~0.15 nmol eGFP/unit of furin/hr) in the amount of free eGFP was observed over 10 h, indicating gradual release of eGFP from the NCs. The slower releasing phase observed before 6 h may be attributed to an initial period in which the peptide CLs are being digested by furin. When an increased concentration of enzyme (4 units) was incubated with NCs, the release of protein occurred more rapidly and reached a similar plateau level corresponding to ~80% total eGFP encapsulated. When a competitive furin inhibitor, dec-RVKR-cmk,[32] was added to the assay (10 μM), the release of eGFP was remarkably attenuated to the same level as the nondegradable and furin-free samples. To assess the stability of NCs, we performed the eGFP release assay of furin-degradable NCs in conditions established for stability studies of nanoparticles, including the uses of an acidic pH 5.5 buffer and a high-salt concentration of 500 mM NaCl.[33,34] As shown in Figure S6, Supporting Information, NCs did not show significant protein release in either of these conditions, indicating the NC remains intact and is not subject to nonspecific acid hydrolysis or destabilization due to shifts in ionic strength. These combined results confirmed that the release of native eGFP from the NCs was specifically dependent on the enzymatic activities of furin.

Intracellular Furin-Mediated Native Protein Delivery in CHO Cell Lines. Having established the furin-dependent degradability of the NCs, we then sought to demonstrate the ability of NCs to delivery native proteins to the nuclei of mammalian cells. The first target protein chosen was eGFP fused with the nuclear localization signal (NLS, sequence PKKKRKV) from the simian virus 40 large-T antigen (NLS-eGFP).[35] NLS-eGFP is chosen as a fluorescent marker for the following reasons: First, NC-mediated delivery into the cytosol of cells can be readily visualized. However, in the absence of NC degradation, the NLS tag will be concealed and thus confine the eGFP fluorescence in the cytosol. Subsequently following furin-mediated degradation of NCs, we expect NLS-eGFP to be released and lead to entry of eGFP into the nucleus facilitated by the exposed NLS tag. The change in the localization of the eGFP signal will then be an indication of the release of protein cargo.

We first compared the extent of nuclear colocalization of delivered NLS-eGFP using different Chinese hamster ovary (CHO) cell lines with varied intracellular furin levels, including CHO-K1 that expresses furin at a normal level, FD11 that is furin-deficient, and FD11 + furin which is the FD11 strain transfected with an overexpressed furin gene.[36] We incubated 200 nM furin-degradable NLS-eGFP NCs with CHO cell lines and examined intracellular delivery with confocal microscopy after 24 h. Localization of eGFP signal to the nucleus was prominent with furin-degradable NCs in CHO-K1 and FD11 + furin cells (Figure 2A). In contrast, eGFP fluorescence was only localized in the cytosol in FD11 cells, and no nuclear entry was observed, indicating no capsule degradation in the absence of furin. Furthermore, when nondegradable NCs were used as

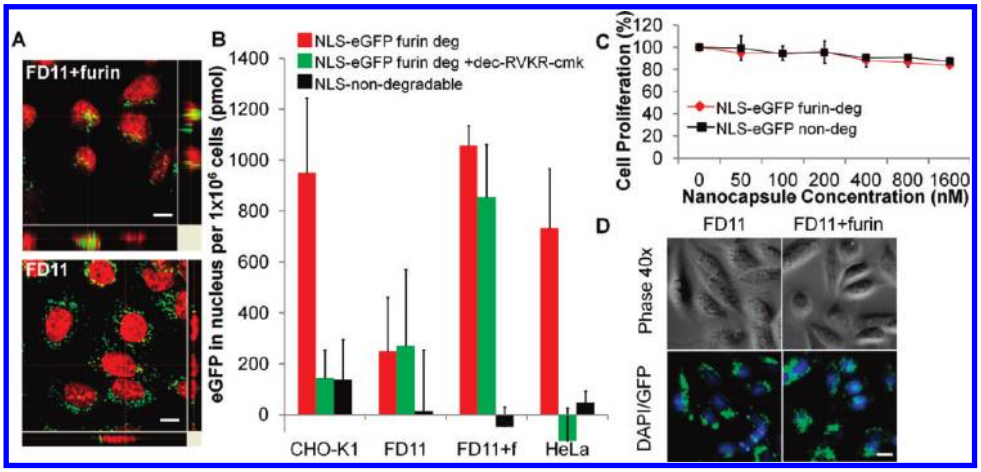

Figure 2. ***In vitro*** **studies demonstrating furin-degradability of NCs. (A) Confocal images of 200 nM furin-degradable NLS-eGFP NCs delivered to FD11 + furin cells and FD11 furin-deficient cells after 24 h treatment; red: nuclei, green: eGFP. The central panel shows a slice of the *xy* plane, the *xz* plane corresponding to the position of the crosshairs is shown on the right, and the *yz* plane is shown at the bottom. The scale bars are 10 μm. (B) Quantification of eGFP in the nuclear fraction of NC-treated cells using ELISA. Cells were treated for 24 h before the nuclei were isolated. The data shown represent the average value with error bars from three independent experiments. (C) Cell proliferation profiles of NCs delivered to CHO-K1 cells for 24 h which were quantified by the MTS assay. (D) Representative phase and fluorescence images of CHO cell lines treated with NLS-eGFP degradable NCs. The scale bar is 100 μm.**

delivery vehicles for NLS-eGFP, nearly all fluorescence was found only in the cytosol for all cell lines (Figure S5, Supporting Information), confirming the inaccessibility of the encapsulated NLS-eGFP toward the nuclei.

To quantify the extent of nuclear delivery of NLS-eGFP, we isolated the nuclear fractions from these treated cells and measured the amount of eGFP using ELISA. As shown in Figure 2B, the levels of eGFP delivered to the nuclei by furin-degradable NCs were two to three times greater in furin-expressing cell lines compared to FD11. When these cells were cocultured with furin-degradable NCs and 25 μM dec-RVKR-cmk, the amount of eGFP in CHO-K1 decreased to that of the FD11 levels. A smaller decrease was observed in FD11 + furin cell lines treated with furin inhibitor, which may be attributed to the higher expression levels of furin. As controls, nearly no nuclear localization of eGFP was observed in: (1) NLS-eGFP delivered by nondegradable NCs; (2) untagged eGFP delivered by furin-degradable NCs; and (3) NLS-eGFP delivered by NCs cross-linked with Ahx-AAARSK (Figure S2, Supporting Information), which is not recognized by furin (Figure S5g, Supporting Information). The absence of nuclear eGFP delivery when NCs were cross-linked with a nonfurin-specific peptide indicates that the peptide CL is not subjected to hydrolysis by nonspecific proteases. Notably, NCs did not show significant cytotoxicity up to ~2 μM in cell lines treated with NLS-eGFP NCs for 24 h (Figure 2C and Figure S9, Supporting Information). Furthermore, FD11 and FD11 + furin cells treated with 400 nM furin-degradable NLS-eGFP NCs displayed identical cell morphologies and no visible toxicity despite different intracellular eGFP localization, further confirming the nontoxic nature of this delivery method (Figure 2D). Thus, proteolytically cleavable NCs can be constructed with specific peptide crossslinkers, and the degradation to release protein can be modulated by the activities of furin or other target endoproteases. Examination of furin-dependent nuclear delivery of eGFP utilizing: (1) CHO cell lines with varying furin concentrations; (2) a competitive furin inhibitor dec-RVKR-cmk; and (3) nonspecific peptide CLs (Ahx-AAARSK) collectively indicates that the presence of active intracellular furin and furin-degradable NCs are both required for successful delivery.

Internalization of Protein NCs in Human Cell Lines. We then explored intracellular protein delivery to various human cell lines. We first studied the delivery of NCs to the HeLa cell line, which exhibits high levels of furin expression.[37] When furin-degradable NLS-eGFP NCs were delivered to HeLa cells, significant eGFP localization was observed within nuclei (Figure S5, Supporting Information). Quantitative analysis of nuclear eGFP levels also confirmed the successful delivery of eGFP to HeLa cells using furin-degradable NCs (Figure 2B). We then explored the cellular trafficking of furin-degradable NLS-eGFP NCs in HeLa cells. We monitored eGFP fluorescence for 2 h following NC incubation with cells by staining early endosomal marker, EEA1, or the late endosomal marker, CI-MPR (Figure 3A). After 30 min incubation, eGFP NCs showed ~60% peak colocalization with EEA1 indicating that NCs are internalized by endocytosis (Figure 3B). The observation of eGFP fluorescence signals at later time points lacking colocalization with either endosomal marker indicates that some NCs or proteins are able to be delivered into the cytosol within 2 h of cellular uptake (Figure 3A and Figure S8, Supporting Information). The inefficient escape of protein from the endosome to the cytosol remains an obstacle in many current delivery

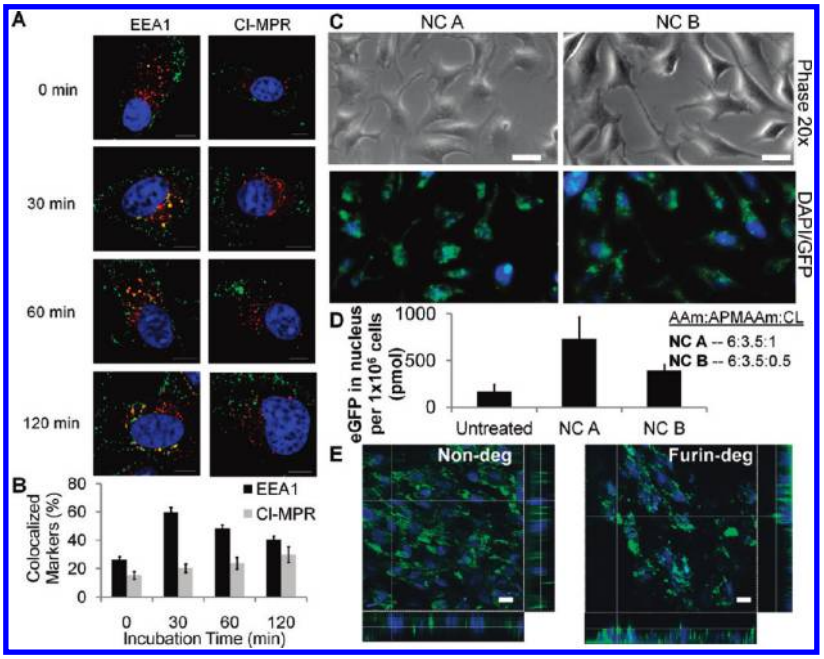

Figure 3. Cellular internalization of NCs in human cell lines. (A) The trafficking of NLS-eGFP NCs through endosomes. Early and late endosomes were detected by EEA1 antibody (left) and CI-MPR antibody (right), respectively, which are stained in red. HeLa cells were incubated with 10 nM NLS-eGFP NCs at 37 °C for various time points, fixed, and the overlap of eGFP with endosomal markers was observed by red and green colocalization resulting in a yellow color. The nuclei are stained with DAPI shown in blue. The scale bar is 10 μm. (B) Quantification of NLS-eGFP NCs colocalized with EEA1 + or CI-MPR + endosomal markers at various incubation times. Colocalization coefficients were calculated using the Manders' overlap coefficient (>10 samples). (C) Phase and fluorescence images of HeLa cells treated with degradable NLS-eGFP NCs for 24 h with varying cross-linking density (blue: DAPI-stained nuclei; green: GFP). NC A was synthesized with twice the amount of furin-degradable CL as NC B. The scale bars are 100 μm. (D) Quantification of eGFP using ELISA in extracted nuclei of HeLa cells treated with NC A and NC B with varying cross-linking densities of NCs. (E) Confocal images of AFDC cells treated with 200 nM nondegradable (left) and furin-degradable (right) NLS-eGFP NCs (blue: Hoescht stained nuclei, green: eGFP). The scale bars are 50 μm.

approaches.[38,39] Delivery methods that rely on cytosolic esterases or reducing environments to release protein may never reach the cytosol and become entrapped in endosomes, undergo lysosomal degradation, and are eventually cleared from the system.

We also used HeLa cells to observe the effects of using various amounts of furin-degradable CL to synthesize NCs. We varied the molar ratio of AAm:APMAAm:CL from 6:3.5:1 (A) to 6:3.5:0.5 (B) and synthesized furin-degradable NLS-eGFP NCs. Both NCs had similar size and charge (Table S1, Supporting Information). As shown in Figure 3C and Figure S8, Supporting Information, cells treated with NCs synthesized with more CL (NC A) displayed higher colocalization with nuclei than those treated with NCs synthesized with less CL (NC B), while the overall internalization of eGFP and cell morphologies were comparable after 24 h. When the nuclear fractions were extracted and eGFP was quantified with ELISA, nuclear eGFP of NC A-treated cells were significantly higher than that of cells treated with NC B (Figure 3D). These results imply that the degradability and the surface chemistry of NCs may play an important role in internalization and may facilitate cytosolic native protein delivery at various cellular entry points.

We then examined protein delivery into human amniotic fluid-derived cells (hAFDCs). hAFDCs have the potential to differentiate into all three germ layers[40] and act as somatic resources which can be efficiently induced into a pluripotent state.[41] Hence, controlled delivery of various factors to tune the functions of these cells has significant therapeutic potential. We delivered furin-degradable and nondegradable NLS-eGFP NCs to hAFDCs and examined the extent of nuclear delivery using confocal microscopy as shown in Figure 3E and Figure S8, Supporting Information. hAFDCs treated with 200 nM furin-degradable NCs show a marked overlap between cell nuclei and protein, while fluorescence signals from nondegradable NCs were only detected in the cytosol. These results strongly indicate that furin-degradable NCs can be used to deliver proteins to the nuclei of a diverse variety of mammalian cells.

Delivery of Anticancer Caspase-3 to HeLa Cells. To further demonstrate the utility of furin-mediated release of functional protein cargo from the degradable NCs, we prepared NCs containing CP3. CP3 is a potent executioner when delivered in native form to cells, as it acts as a signal peptidase in the cellular apoptotic pathway.[42,43] Therefore, cell apoptosis is the physiological change observed upon successful delivery and release of native CP3 protein. We previously delivered CP3 to cells using self-degradable NCs cross-linked with CP3-cleavable peptides;[22] here we seek to generalize the

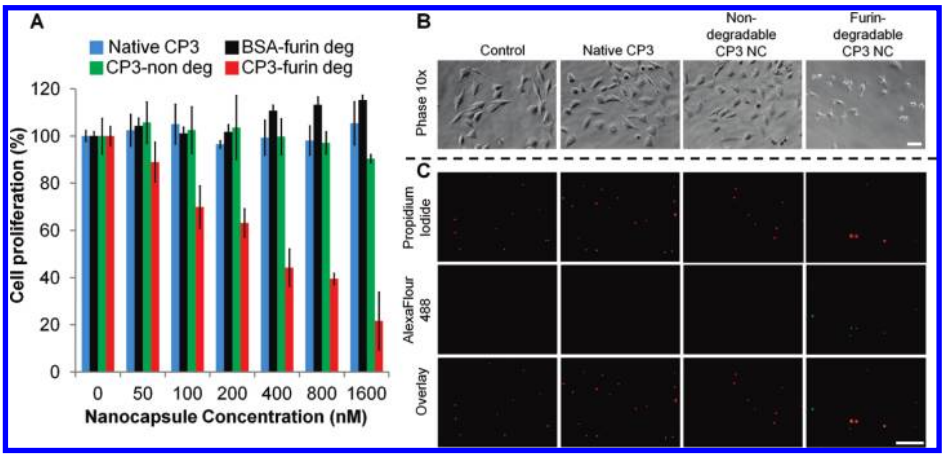

Figure 4. Cytosolic delivery of caspase-3 to HeLa cells. (A) Cell death profiles of HeLa cells treated with various cross-linked NCs/protein for 24 h before performing the MTS assay for quantification of cell proliferation. (B) Cell phase images prior to the TUNEL assay of HeLa cells treated with NCs for 24 h. The scale bar is 200 μm. (C) TUNEL assay results following detachment of NC-treated cells, permeabilization, and staining. Propidium iodide (red) signifies the total DNA content, while AlexaFluor 488-tagged antibody (green) corresponds to nick end DNA. The scale bar is 200 μm.

degradability of that system by utilizing the activities of intracellular furin instead. CP3 NCs were prepared in similar fashion as the eGFP NCs starting from purified, recombinant CP3. Various control CP3 NCs were also synthesized to facilitate comparison to the furin-degradable vehicle. After confirmation of surface charges and sizes (Table S1, Supporting Information), the CP3 NCs were added to HeLa cells. As shown in Figure 4A, cell death was only observed in HeLa cells treated with furin-degradable CP3 NCs, with IC_{50} of ~400 nM. In contrast, cells treated with unencapsulated native CP3, nondegradable NCs, and furin-degradable BSA NCs all exhibited minimal apoptotic death within the concentrations of NCs used, confirming the furin-dependent release of CP3 and the relatively nontoxic nature of the polymeric capsule. This indicates that only furin-degradable CP3 NCs are able both to enter the cell and be degraded to release the executioner protein which can induce apoptosis. To confirm the cell death observed was indeed apoptosis, we performed the terminal deoxynucleotidyl transferase dUTP nick end labeling (TUNEL) assay which detects DNA fragmentation by labeling the terminal end of nucleic acids.[44] When cells were treated with 200 nM CP3 NCs or protein, trademark cell membrane blebbing and shrinkage characteristics of apoptotic cells were observed in cells treated with furin-degradable CP3 NCs (Figure 4B). After detachment of cells and performance of the TUNEL assay, detection of DNA nicks observed with AlexaFlour488-labeled antibody (green) was only detected in cells treated with furin-degradable CP3 NCs (Figure 4C and Figure S8, Supporting Information). In contrast, native CP3-treated cells or nondegradable CP3 NC-treated cells did not show signals of nicked DNA in the total DNA content visualized with propidium iodide (red). This indicates that furin-degradable NCs are able to deliver active CP3 to the cytosol and lead to apoptosis.

The successful delivery of CP3 also implicates the future potential of this system to deliver various cancer therapeutics which can interact with cellular machinery to activate the apoptotic pathway.[45] The amount of furin-degradable CLs incorporated in the NC can be tuned to achieve cell-specific intracellular protein delivery, as furin is upregulated in breast, ovary, head and neck, and brain as well as nonsmall cell lung carcinomas, in comparison to normal cells.[46−49] In this study, a positive surface charge on the NC was targeted to facilitate cellular entry by interaction with the negatively charged phospholipid bilayer membrane.[50] To achieve selective cellular uptake, targeting positive ligands could be attached to the surface of the NCs, and the surface charge could be adjusted to neutral by using uncharged monomers.[51]

Delivery of a Transcription Factor to Nuclei of MEF Cells. To demonstrate the delivery of biologically relevant nuclear protein cargos to cells, we prepared NCs encapsulating the transcription factor Klf4. Klf4 is critical in regulating expression levels of genes involved in maintaining the cell cycle as well as cellular structure, adhesion, metabolism, and signaling.[52] Many studies implicate Klf4 as a tumor suppressor for colorectal and gastric cancers.[53] Particularly, Klf4 has been shown to be one of the essential factors needed to maintain a pluripotent state.[54] Recently, recombinant iPS transcription factor proteins were fused to protein transduction domains (PTDs) of multiple arginines (9R or 11R), transduced into mouse and human fibroblasts, and reprogrammed to produce induced pluripotent stem (iPS) cells.[55,56] The 11R-tagged proteins have been delivered *in vitro* and *in vivo* to subcellular compartments, such as nuclei and mitochondria in a variety of tissues and organs, including the brain, heart, and lymphocytes, thereby asserting 11R tags as a useful delivery strategy for protein therapeutics.[57] We sought to compare intracellular delivery of

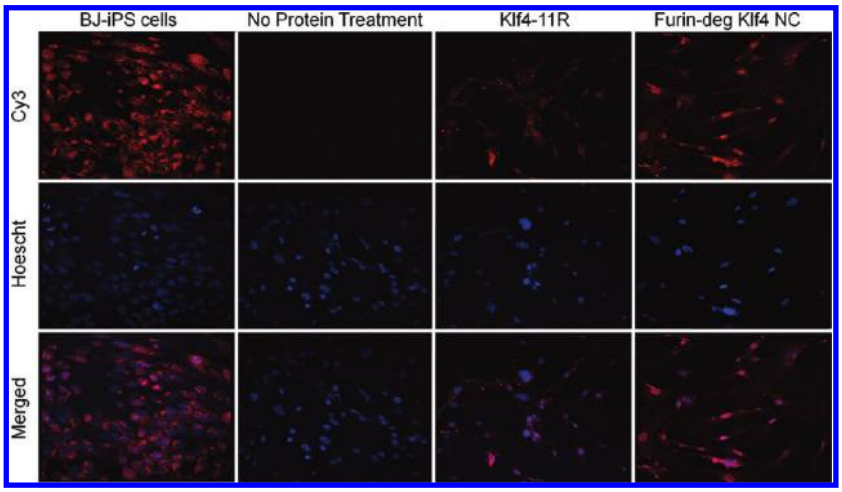

Figure 5. Intracellular delivery of Klf4 to cells. Klf4 immunostaining in MEF cultures treated with Klf4-11R and furin-degradable Klf4 NCs was examined using confocal imaging. BJ-iPSCs were also immunostained as a positive control, and cells without any treatment were used as a negative control. The top panel shows Klf4 immunostaining with Cy3 conjugated antibody (red), middle panel shows nuclear staining using Hoescht dye (blue), and bottom panel shows overlap between both.

11R-tagged proteins and protein NCs using Klf4 as a model.

We synthesized NCs with Klf4-11R and verified the size of nanocapsules to be ~20 nm with TEM (Figure S10, Supporting Information). We directly determined the extent of protein delivery by performing immunocytochemistry after culturing mouse embryonic fibroblast (MEF) cells with Klf4-11R or furin-degradable Klf4 NCs. As shown in Figures 5 and Figure S8, Supporting Information, Klf4 delivered via NC can be prominently detected in nuclei of cells which are counterstained with Hoescht and examined using confocal microscopy. Virtually every cell nucleus shows a strong signal of Klf4 staining. The degree of staining is comparable to the positive control, BJ-iPS cells, which are neonatal human foreskin fibroblasts which have been reprogrammed into iPS cells and have high-expression levels of Klf4.[58] In contrast, Klf4-11R shows much weaker intensity and much less colocalization with nuclei indicating delivery of Klf4 was not as efficient. PTD-tagged cargo often becomes trapped in endosomal compartments with no mechanism of release into the cytosol, and <1% of the protein cargo may be released.[4,59] The prominent staining of Klf4 in the nuclei of MEF cells suggests that NCs may offer more protection for preservation of protein structure and activity. PTD-tagged proteins and other proteins which are exposed to the acidic environment in the endosome often experience degradation and loss of activity. The cargo can also be degraded or subjected to proteolysis during cellular entry. In contrast, the endoprotease-mediated delivery system has a protective polymer layer during cellular uptake until cleavage by furin and release of protein. Collectively, these findings demonstrate that degradable nanocapsules are suitable vehicles for nuclear delivery for transcription factors. The successful nuclear delivery of Klf4 using furin-degradable NCs is also particularly promising as a reprogramming tool. Direct delivery of transcription factors would allow patient-specific therapies which eliminate risks arising from genetic-based methods, including unexpected modifications in target cell genomes.

CONCLUSION

Intracellular delivery of active proteins is an essential goal in various medical applications, including cancer therapy, imaging, vaccination, and treating loss of functioning genes in many diseases.[60] Protein-based therapeutic methods are safer alternatives to gene therapies because no random or permanent genetic changes are involved and only transient actions of proteins are required for desired effects. However, most native proteins are unable to penetrate the cell membrane and often suffer from loss of function due to proteolysis or aggregation in serum. Consequently, a general intracellular protein delivery system is highly desirable for delivery of diverse targets which have different therapeutic uses. Particularly, using an enzymatic-based method would achieve a level of specificity and control which is challenging with current methods.

We successfully demonstrated both cytosolic and nuclear delivery of proteins using our engineered NC carrier which degrades in response to the ubiquitous endoprotease furin. Different cell lines were demonstrated to be amenable hosts for furin-mediated delivery, including the immortalized HeLa, the highly regenerative hAFDC, and the essential structural MEF. We also showed that protein cargos of different sizes and tertiary structures can be encapsulated and released reversibly without loss of bioactivity, including the 27 kDa β-barrel eGFP,[61] the 51 kDa Klf4 that has three zinc finger regions,[62] and the 64 kDa CP3 which is

a heterotetramer.[63] In summary, through extensive imaging and quantitative analysis *in vitro*, we have shown the successful delivery of both cytosolic and nuclear proteins based on specific furin-mediated degradation and cargo release. This approach may also be applicable to the intracellular delivery of other therapeutics, including small drugs, peptides, siRNA, and plasmid DNA.

MATERIALS AND METHODS

Complete materials and methods can be found in the Supporting Information.

Synthesis of Furin-Degradable Peptide. Peptides were synthesized using an automatic peptide synthesizer. Standard solid-phase peptide synthesis protocols for Fmoc chemistry were used. Peptides were assembled in the C-terminal amide form using rink amide 4-methylbenzhydrylamine (MBHA) resins (Anaspec, Inc.). Coupling of amino acids to the resin backbone was accomplished by a 0.9 equiv of 2-(1H-benzotriazole-1-yl)-1,1,3,3-tetramethyluronium hexafluorophosphate (HBTU) activation and 2 equiv of diisopropylethylamine (DIEA). The Fmoc group was removed by 20% piperidine in dimethylformamide (DMF). Peptides were constructed with Fmoc-6-Ahx-OH at the N-terminal and Fmoc-Lys(Mtt)-OH at the C-terminal (Ahx-RVRRSK). The nonspecific peptide (Ahx-AAARSK) was constructed in the same manner.

Resin bearing peptides were swollen in DCM, and then the Mtt group was selectively removed with 3% TFA in DCM. The exposed primary amine groups were acrylolated using a 20-fold excess of acryloyl chloride and 20-fold excess of DIEA in DMF for 1 h on ice and then 1 h at room temperature. The progress of acrylolation was monitored with the *p*-chloranil test. When a negative *p*-chloranil test was achieved, the resin was washed, dried under vacuum, and cleaved using TFA:water:TIPS in a 95:2.5:2.5 ratio. After cleavage, the peptide was drained into cold ether, washed, and centrifuged four times. The crude peptide was dissolved in water and lyophilized. The nonspecific peptide was constructed in the same manner.

Preparation of Protein NCs. One mg protein was diluted to 1 mL with 5 mM pH 9 $NaHCO_3$ buffer after which acrylamide (AAm) was added with stirring for 10 min at 4 °C. Next, *N*-(3-aminopropyl) methacrylamide (APMAAm) was added. Afterward, the peptide CL or nondegradable CL *N*,*N*′-methylene bisacrylamide was added. The molar ratio of AAm:APMAAm:CL was 6:3.5:1. The polymerization was immediately initiated by adding 3 mg of ammonium persulfate and 3 μL of *N*,*N*,*N*′,*N*′-tetramethylethylenediamine. The polymerization was allowed to proceed for 90 min at 4 °C. Finally, buffer exchange with 100 mM 4-(2-hydroxyethyl)-1-piperazineethanesulfonic acid (HEPES) and 1 mM $CaCl_2$, pH 7.5, was performed to remove unreacted monomers and initiators.

Cell Free Furin Cleavage of Peptide and NCs. Fifty ng of furin CL peptide or 2.5 nmol of furin-degradable protein NCs was added to 100 mM HEPES, 1 mM $CaCl_2$, and pH 7.5 buffer to a total volume of 40 μL. One unit of furin enzyme was added to the reaction mixture and incubated at 37 °C for various times. One unit of enzyme is defined by Sigma as the amount of enzyme needed to release 1 pmole from flourogenic peptide Boc-RVRR-AMC in 1 min at 30 °C. When furin inhibitor dec-RVKR-cmk (EMD Chemicals, Inc., Gibbstown, NJ) was used, it was added to the reaction mixture at a final concentration of 25 μM.

Enzyme-linked Immunosorbant Assay (ELISA). To quantify native eGFP protein released, a GFP ELISA kit was purchased from Cell Biolabs, Inc., San Diego, CA. We constructed a standard curve by using known eGFP amounts with the kit's standard eGFP sample and by performing the assay. Briefly, samples were centrifuged for 10 min at 7000 rpm with a 30 kDa molecular weight cut-off (MWCO) filter to isolate native eGFP protein. Then, the samples were loaded into anti-GFP rabbit antibody coated wells and incubated at 4 °C overnight. After careful washing, a detection antibody (anti-GFP mouse antibody) was added to each well and incubated at room temperature for 2 h. Next, an anti IgG mouse-HRP conjugate antibody was added. After 1 h, tetramethylbenzidine (TMB) substrate was added and incubated for 30 min. After the addition of stop solution to each well, absorbance at 450 nm was measured.

Cell Culture. HeLa, MEF, (ATCC, Manassas, VA), and CHO cells (a generous gift from Stephan Leppla, National Institutes of Health) were cultured in Dulbecco's modified eagle's medium (DMEM, Invitrogen) supplemented with 10% bovine growth serum (BGS, Hyclone, Logan, UT), 1.5 g/L sodium bicarbonate, 100 μg/mL streptomycin, and 100 U/mL penicillin. AFDC cells were cultured in minimum essential medium (α-MEM; Invitrogen) supplemented with 10% fetal bovine serum (FBS). The cells were cultured at 37 °C, in 98% humidity and 5% CO2. Cells were regularly subcultured using trypsin-ethylenediaminetetraacetic acid (EDTA).

Cellular Internalization Trafficking. NLS-eGFP NCs (10 nM) were added to HeLa cells at 4 °C for 30 min. The cells were shifted to 37 °C for various incubation periods, fixed with 4% formaldehyde, permeabilized with 0.1% triton X-100, and separately immunostained with antibodies against early endosomes (mouse anti-EEA1 Ab) and late endosomes (rabbit anti-CI-MPR Ab). Texas red goat anti-mouse IgG and Alexa Fluor647 goat anti-rabbit IgG were used as secondary antibodies. The nuclei of treated cells were stained with DAPI. To quantify the extent of colocalization between eGFP and endosomes, colocalization coefficients were calculated using the Manders' overlap coefficient by viewing more than 10 cells at each time point using the Nikon NIS-Elements software.

Nuclear and Cytoplasmic Fractionation. Cells were seeded into 6-well plates at a density of 1×10^5 cells per well and cultivated in 1.5 mL of DMEM with 10% BGS. The plates were incubated in 5% CO_2 and at 37 °C for 12 h before being treated with 200 nM of appropriate NCs. Dec-RVKR-cmk was used at a concentration of 25 μM. Cells were collected by trypsin-EDTA and by centrifugation after 24 h. A nuclear/cytosol fractionation kit (BioVision, Inc., Mountain View, CA) was used to separate cytoplasmic and nuclear extracts from NC-treated cells. Fractions were obtained per the manufacturer's instructions. All procedures were performed at 4 °C. Extracts were stored at −80 °C until the GFP-ELISA assay was performed (Cell Biolabs, Inc., San Diego, CA). For nuclear staining and subsequent Z-stack imaging, nuclei were counterstained with TO-PRO-3 (Invitrogen).

TUNEL Assay. Apoptosis was detected in isolated HeLa cells using a commercially available APO-BrdU terminal deoxynucleotidyl transferase dUTP nick end labeling (TUNEL) assay kit from Invitrogen. Briefly, cells were seeded into 6-well plates at a density of 100 000 cells per well and cultivated in 2 mL of DMEM with 10% BGS. The plates were then incubated in 5% CO_2 and at 37 °C for 12 h to reach 70−80% confluency before addition of protein/nanocapsules. After 24 h incubation, cells were first fixed with 1% paraformaldehyde in phosphate-buffered saline, pH 7.4, followed by treatment with 70% ethanol on ice to permeabilize the membrane. The cells were then loaded with DNA labeling solution containing terminal deoxynucleotidyl transferase and bromodeoxyuridine (BrdUrd). Cells were then stained with Alexa Fluor 488 dye-labeled anti-BrdUrd antibody for nick end labeling. The cells were finally stained with propidium iodide (PI) solution containing RNase A for total DNA content and visualized under fluorescence microscope (Zeiss, Observer Z1) using appropriate filters for Alexa Fluor 488 and PI.

Immunostaining. Mouse embryonic fibroblast (MEF) cells were plated in 8-well chamber slides at a density of 10 000 cells/well. Cells were treated with 8 μg/mL of Klf4-11R or furin-degradable Klf4 for 6 h and subsequently cultured in fresh media overnight. As a control, BJ-iPS cells were also cultured. Cells were then washed with PBS and fixed by 4% paraformaldehyde in PBS.

Immunostaining was performed with rabbit anti-KLF antibody (1:1000, Santa Cruz Biotechnology, Santa Cruz, CA) and Cy3 conjugated secondary Ab. Hoechst was used for nuclear counterstaining.

Acknowledgment. This work was supported by the David and Lucile Packard Foundation (Y.T.), a Broad Stem Cell Research Center Research Award (G.F.), and an NSF Graduate Fellowship (A.B.). We thank Dr. Leppla for CHO cell lines, Dr. Huang for use of the SPPS synthesizer, Dr. Clark for pHC332, and Dr. Quinn Ng for assistance with confocal imaging.

Supporting Information Available: Additional experimental procedures, Table S1, Scheme S1 and Figures S1−S10. This material is available free of charge *via* the Internet at http://pubs.acs.org.

REFERENCES AND NOTES

1. Leader, B.; Baca, Q. J.; Golan, D. E. Protein Therapeutics: A Summary and Pharmacological Classification. *Nat. Rev. Drug Discovery* **2008,** *7*, 21–39.
2. Kabanov, A. V.; Vinogradov, S. V. Nanogels as Pharmaceutical Carriers: Finite Networks of Infinite Capabilities. *Angew. Chem., Int. Ed.* **2009,** *48*, 5418–5429.
3. Schwarze, S. R.; Hruska, K. A.; Dowdy, S. F. Protein Transduction: Unrestricted Delivery into All Cells?. *Trends Cell Biol.* **2000,** *10*, 290–295.
4. Murriel, C.; Dowdy, S. Influence of Protein Transduction Domains on Intracellular Delivery of Macromolecules. *Expert Opin. Drug Delivery* **2006,** *3*, 739–746.
5. Diwan, M.; Park, T. G. Pegylation Enhances Protein Stability During Encapsulation in PLGA Microspheres. *J. Controlled Release* **2001,** *73*, 233–244.
6. Lee, Y.; Fukushima, S.; Bae, Y.; Hiki, S.; Ishii, T.; Kataoka, K. A Protein Nanocarrier from Charge-Conversion Polymer in Response to Endosomal pH. *J. Am. Chem. Soc.* **2007,** *129*, 5362–5363.
7. Lee, Y.; Ishii, T.; Cabral, H.; Kim, H. J.; Seo, J.; Nishiyama, N.; Oshima, K.; Osada, K.; Kataoka, K. Charge-Conversional Polyionic Complex Micelles-Efficient Nanocarriers for Protein Delivery into Cytoplasm. *Angew. Chem., Int. Ed.* **2009,** *48*, 5309–5312.
8. Ayame, H.; Morimoto, N.; Akiyoshi, K. Self-Assembled Cationic Nanogels for Intracellular Protein Delivery. *Bioconjugate Chem.* **2008,** *19*, 882–890.
9. Rivera-Gil, P.; De Koker, S.; De Geest, B. G.; Parak, W. J. Intracellular Processing of Proteins Mediated by Biodegradable Polyelectrolyte Capsules. *Nano Lett.* **2009,** *9*, 4398–4402.
10. Dalkara, D.; Chandrashekhar, C.; Zuber, G. Intracellular Protein Delivery with A Dimerizable Amphiphile for Improved Complex Stability And Prolonged Protein Release in The Cytoplasm of Adherent Cell Lines. *J. Controlled Release* **2006,** *116*, 353–359.
11. Akagi, T.; Wang, X.; Uto, T.; Baba, M.; Akashi, M. Protein Direct Delivery to Dendritic Cells Using Nanoparticles Based on Amphiphilic Poly(Amino Acid) Derivatives. *Biomaterials* **2007,** *28*, 3427–3436.
12. Peer, D.; Karp, J. M.; Hong, S.; Farokhzad, R. M.; Langer, R. Nanocarriers As An Emerging Platform for Cancer Therapy. *Nat. Nanotechnol.* **2007,** *2*, 751–760.
13. Gao, J. H.; Xu, B. Applications of Nanomaterials inside Cells. *Nano Today* **2009,** *4*, 37–51.
14. Murthy, N.; Xu, M.; Schuck, S.; Kunisawa, J.; Shastri, N.; Fréchet, J. M. A Macromolecular Delivery Vehicle for Protein-Based Vaccines: Acid-Degradable Protein-Loaded Microgels. *Proc. Natl. Acad. Sci. U.S.A* **2003,** *100*, 4995–5000.
15. Bachelder, E. M.; Beaudette, T. T.; Broaders, K. E.; Dashe, J; Frechet, J. M. J. Acetal-Derivatized Dextran: An Acid-Responsive Biodegradable Material for Therapeutic Applications. *J. Am. Chem. Soc.* **2008,** *130*, 10494–10495.
16. Bauhuber, S.; Hozsa, C.; Breunig, M.; Gopferich, A. Delivery of Nucleic Acids *Via* Disulfide-Based Carrier Systems. *Adv. Mater.* **2009,** *21*, 3286–3306.
17. Sullivan, C. O.; Birkinshaw, C. *In Vitro* Degradation of Insulin-Loaded Poly(N-Butylcyanoacrylate) Nanoparticles. *Biomaterials* **2004,** *25*, 4375–4382.
18. Hasadsri, L.; Kreuter, J.; Hattori, H.; Iwasaki, T.; George, J. M. Functional Protein Delivery into Neurons Using Polymeric Nanoparticles. *J. Biol. Chem.* **2009,** *284*, 6972–6981.
19. Ulijn, R. V. Enzyme-Responsive Materials: A New Class of Smart Biomaterials. *J. Mater. Chem.* **2006,** *16*, 2217–2225.
20. Lei, Y. G.; Segura, T. DNA Delivery from Matrix Metalloproteinase Degradable Poly(ethylene glycol) Hydrogels to Mouse Cloned Mesenchymal Stem Cells. *Biomaterials* **2009,** *30*, 254–265.
21. Adeloew, C.; Segura, T.; Hubbell, J. A.; Frey, P. The Effect of Enzymatically Degradable Poly(ethylene glycol) Hydrogels on Smooth Muscle Cell Phenotype. *Biomaterials* **2008,** *29*, 314–326.
22. Gu, Z.; Yan, M.; Hu, B.; Joo, K.; Biswas, A.; Huang, Y.; Lu, Y.; Wang, P.; Tang, Y. Protein Nanocapsule Weaved with Enzymatically Degradable Polymeric Network. *Nano Lett.* **2009,** *9*, 4533–4538.
23. Seidah, N. G.; Day, R.; Marcinkiewicz, M.; Chretien, M. Precursor Convertases: An Evolutionary Ancient, Cell-Specific, Combinatorial Mechanism Yielding Diverse Bioactive Peptides And Proteins. *Ann. N.Y. Acad. Sci.* **1998,** *839*, 9–24.
24. Krysan, D. J.; Rockwell, N. C.; Fuller, R. S. Quantitative Characterization of Furin Specificity- Energetics of Substrate Discrimination Using An Internally Consistent Aet of Hexapeptidyl Methylcoumarinamides. *J. Biol. Chem.* **1999,** *274*, 23229–23234.
25. Thomas, G. Furin at The Cutting Edge: From Protein Traffic to Embryogenesis And Disease. *Nat. Rev. Mol. Cell. Biol.* **2002,** *3*, 753–766.
26. Richards, R. M.; Lowy, D. R.; Schiller, J. T.; Day, P. M. Cleavage of The Papillomavirus Minor Capsid Protein, L2, at A Furin Consensus Site Is Necessary for Infection. *Proc. Natl. Acad. Sci. U.S.A.* **1998,** *103*, 1522–1527.
27. Youker, R. T.; Shinde, U.; Day, R.; Thomas, G. At The Crossroads of Homoeostasis And Disease: Roles of The PACS Proteins in Membrane Traffic And Apoptosis. *Biochem. J.* **2009,** *421*, 1–15.
28. Plunkett, K. N.; Berkowski, K. L.; Moore, J. S. Chymotrypsin Responsive Hydrogel: Application of a Disulfide Exchange Protocol for the Preparation of Methacrylamide Containing Peptides. *Biomacromolecules* **2005,** *6*, 632–637.
29. OBrienSimpson, N. M.; Ede, N. J.; Brown, L. E.; Swan, J.; Jackson, D. C. Polymerization of Unprotected Ssynthetic Peptides: A View Toward Synthetic Peptide Vaccines. *J. Am. Chem. Soc.* **1997,** *119*, 1183–1188.
30. Gu, Z.; Biswas, A.; Joo, K.; Hu, B.; Wang, P.; Tang, Y. Probing Protease Activity by Single-Fluorescent-Protein Nnanocapsules. *Chem. Comm.* **2010,** *46*, 6467–6469.
31. Mansouri, S.; Cuie, Y.; Winnik, F.; Shi, Q.; Lavigne, P.; Benderdour, M.; Beaumont, E.; Fernandes, J. C. Characterization of Folate-Chitosan-DNA Nanoparticles for Gene Therapy. *Biomaterials* **2006,** *27*, 2060–2065.
32. Jean, F.; Stella, K.; Thomas, L.; Liu, G.; Xiang, Y.; Reason, A. J. Thomas G. Alpha(1)-Antitrypsin Portland, A Bioengineered Serpin Highly Selective for Furin: Application As An Antipathogenic Agent. *Proc. Natl. Acad. Sci. U.S.A.* **1998,** *95*, 7293–7298.
33. Jin, R. C.; Wu, G. S.; Li, Z.; Mirkin, C. A.; Schatz, G. C. What Controls The Melting Properties of DNA-Linked Gold Nanoparticle Assemblies?. *J. Am. Chem. Soc.* **2003,** *125*, 1643–1654.
34. Mei, B. C.; Susumu, K.; Medintz, I. L.; Mattoussi, H. Polyethylene Glycol-Based Bidentate Ligands to Enhance Quantum Dot And Gold Nanoparticle Stability in Biological Media. *Nat. Protoc.* **2009,** *4*, 412–423.
35. Hodel, M. R.; Corbett, A. H.; Hodel, A. E. Dissection of A Nuclear Localization Signal. *J. Biol. Chem.* **2001,** *276*, 1317–1325.
36. Gordon, V. M.; Klimpel, K. R.; Arora, N.; Henderson, M. A.; Leppla, S. H. Proteolytic Activation of Bacterial Toxins by Eukaryotic Cells Is Performed by Furin and by Additional Cellular Proteases. *Infect. Immun.* **1995,** *63*, 82–87.

37. Page, R. E.; Klein-Szanto, A. J.; Litwin, S.; Nicolas, E.; Al-Jumaily, R.; Alexander, P.; Godwin, A. K.; Ross, E. A.; Schilder, R. J. Increased Expression of The Pro-Protein Convertase Furin Predicts Decreased Survival in Ovarian Cancer. *Cell. Oncol.* **2007,** *29*, 289–299.
38. Torchilin, V. P. Recent Approaches to Intracellular Delivery of Drugs And DNA And Organelle Targeting. *Annu. Rev. Biomed. Eng.* **2006,** *8*, 343–375.
39. Hoffman, A. S.; Stayton, P. S.; Press, O.; Murthy, N.; Lackey, C. A.; Cheung, C.; Black, F.; Campbell, J.; Fausto, N.; Kyriakides, T. R. Design of "Smart" Polymers That Can Direct Intracellular Drug Delivery. *Polymer Adv. Tech.* **2002,** *13*, 992–999.
40. Toda, A.; Okabe, M.; Yoshida, T.; Nikaido, T. The Potential of Amniotic Membrane/Amnion-Derived Cells for Regeneration of Various Tissues. *J. Pharmacol. Sci.* **2007,** *105*, 215–228.
41. Li, C. L.; Zhou, J.; Shi, G.; Ma, Y.; Yang, Y.; Gu, J.; Yu, H.; Jin, S.; Wei, Z.; Chen, F. Pluripotency Can Be Rapidly And Efficiently Induced in Human Amniotic Fluid-Derived Cells. *Hum. Mol. Genet.* **2009,** *18*, 4340–4349.
42. Cotter, T. G. Apoptosis And Cancer: The Genesis of A Research Field. *Nat. Rev. Cancer* **2009,** *9*, 501–507.
43. Riedl, S. J.; Renatus, M.; Schwarzenbacher, R.; Zhou, Q.; Sun, C.; Fesik, S. W.; Liddington, R. C.; Salvesen, G. S. Structural Basis for The Inhibition of Caspase-3 by XIAP. *Cell* **2001,** *104*, 791–800.
44. Gavrieli, Y.; Sherman, Y.; Bensasson, S. A. Identification of Programmed Cell-Death *In Situ Via* Specific Labeling of Nuclear-DNA Fragmentation. *J. Cell. Biol.* **1992,** *119*, 493–501.
45. Bale, S. S.; Kwon, S. J.; Shah, D. A.; Banerjee, A.; Dordick, J. S.; Kane, R. S. Nanoparticle-Mediated Cytoplasmic Delivery of Proteins To Target Cellular Machinery. *ACS Nano* **2010,** *4*, 1493–1500.
46. Cheng, M.; Watson, P. H.; Paterson, J. A.; Seidah, N.; Chrétien, M.; Shiu, R. P. Pro-Protein Convertase Gene Expression in Human Breast Cancer. *Int. J. Cancer* **1997,** *71*, 966–971.
47. Bassi, D. E.; Mahloogi, H.; Al-Saleem, L.; De Cicco, R. L.; Ridge, J. A.; Klein-Szanto, A. J. P. Elevated Furin Expression in Aggressive Human Head And Neck Tumors And Tumors Cell Lines. *Mol. Carcinog.* **2001,** *31*, 224–232.
48. Mercapide, J.; De Cicco, R. L.; Bassi, D. E.; Castresana, J. S.; Thomas, G.; Klein-Szanto, A. J. P. Inhibition of Furin-Mediated Processing Results in Suppression of Astrocytoma Cell Growth And Invasiveness. *Clin. Cancer Res.* **2002,** *8*, 1740–1746.
49. Schalken, J. A.; Roebroek, A. J.; Oomen, P. P.; Wagenaar, S. S.; Debruyne, F. M.; Bloemers, H. P.; Van de Ven, W. J. Fur Gene-Expression As A Discriminating Marker for Small-Cell And Nonsmall Cell Lung Carcinomas. *J. Clin. Invest.* **1987,** *80*, 1545–1549.
50. Pack, D. W.; Hoffman, A. S.; Pun, S.; Stayton, P. S. Design And Development of Polymers for Gene Delivery. *Nat. Rev. Drug Discovery* **2005,** *4*, 581–593.
51. Aguilera, T. A.; Olson, E. S.; Timmers, M. M.; Jiang, T.; Tsien, R. Y. Systemic *In Vivo* Distribution of Activatable Cell Penetrating Peptides Is Superior to That of Cell Penetrating Peptides. *Integr. Biol.* **2009,** *1*, 371–381.
52. Rowland, B. D.; Peeper, D. S. KLF4, P21 And Context-Dependent Opposing Forces in Cancer. *Nat. Rev. Cancer* **2006,** *6*, 11–23.
53. Wei, D. Y.; Kanai, M.; Huang, S. Y.; Xie, K. P. Emerging Role of KLF4 in Human Gastrointestinal Cancer. *Carcinogenesis* **2006,** *27*, 23–31.
54. Yu, J. Y.; Vodyanik, M. A.; Smuga-Otto, K.; Anteosiewicz-Bourget, J.; Franel, J. L.; Tian, S.; Nie, J.; Jonsdottir, G. A.; Ruotti, V.; Stewart, R. Induced Pluripotent Stem Cell Lines Derived from Human Somatic Cells. *Science* **2007,** *318*, 1917–1920.
55. Kim, D.; Kim, C. H.; Moon, J. I.; Chung, Y. G.; Chang, M. Y.; Han, B. S.; Ko, S.; Yang, E.; Cha, K. Y.; Lanza, R. Generation of Human Induced Pluripotent Stem Cells by Direct Delivery of Reprogramming Proteins. *Cell Stem Cell* **2009,** *4*, 472–476.
56. Zhou, H. Y.; Wu, S.; Joo, J. Y.; Zhu, S.; Han, D. W.; Lin, T.; Trauger, S.; Bien, G.; Yao, S.; Zhu, Y. Generation of Induced Pluripotent Stem Cells Using Recombinant Proteins. *Cell Stem Cell* **2009,** *4*, 581–581.
57. Matsui, H.; Tomizawa, K.; Lu, Y. F.; Matsushita, M. Protein Therapy: *In Vivo* Protein Transduction by Polyarginine (11R) PTD And Subcellular Targeting Delivery. *Curr. Protein Pept. Sci.* **2003,** *4*, 151–157.
58. Park, I. H.; Zhao, R.; West, J. A.; Yabuuchi, A.; Huo, H.; Ince, T. A.; Lerou, P. H.; Lensch, M. W.; Daley, G. Q. Reprogramming of Human Somatic Cells to Pluripotency With Defined Factors. *Nature* **2008,** *451*, 141–U141.
59. Joliot, A.; Prochiantz, A. Transduction Peptides: From Technology to Physiology. *Nat. Cell Biol.* **2004,** *6*, 189–196.
60. Walsh, G. Biopharmaceutical Benchmarks 2006. *Nat. Biotechnol.* **2006,** *24*, 769–U765.
61. Ormo, M.; Cubitt, A. B.; Kallio, K.; Gross, L. A.; Tsien, R. Y.; Remington, S. J. Crystal Structure of The Aequorea Victoria Green Fluorescent Protein. *Science* **1996,** *273*, 1392–1395.
62. Katz, J. P.; Perreault, M.; Goldstein, B. J.; Lee, C. S.; Labosky, P. A.; Yang, V. W.; Kaestner, K. H. The Zinc-Finger Transcription Factor Klf4 Is Required for Terminal Differentiation of Goblet Cells in The Colon. *Development* **2002,** *129*, 2619–2628.
63. Nicholson, D. W. Caspase Structure, Proteolytic Substrates, And Function During Apoptotic Cell Death. *Cell Death Di□er.* **1999,** *6*, 1028–1042.